

## X-RAY DIFFRACTION AND PHOTOCATALYTIC ACTIVITY OF NATURAL MEXICAN CLINOPTILOLITE

---

*José Manuel Sanchez Viveros*

Instituto Politécnico Nacional, Departamento  
de Física, Ciudad de México, México

*Gregorio Zacahua Tlacuatl*

Instituto Politécnico Nacional, Laboratorio  
de Posgrado, Ciudad de México, México

*Estela Márquez Ramírez*

Universidad Autónoma Metropolitana,  
Departamento de Energía, Ciudad de  
México, México

*Isaías Hernández Pérez*

Universidad Autónoma Metropolitana,  
Departamento de Ciencias Básicas, Ciudad  
de México, México

*Fernando Chávez Rivas*

Instituto Politécnico Nacional, Departamento  
de Física, Ciudad de México, México

*Vitalii Petranovskii*

Universidad Nacional Autónoma de México,  
Departamento de Nanocatálisis, Ensenada,  
Baja California, México

All content in this magazine is licensed under a Creative Commons Attribution License. Attribution-Non-Commercial-Non-Derivatives 4.0 International (CC BY-NC-ND 4.0).



**Abstract:** We present the structural characterization of several sets of minerals: a) natural clinoptilolite (ZNM), b) ZNM subjected to grinding for three hours (ZNM025), c) ZNM025 calcined at 250 °C (ZNM250) and d) ZNM025 treated at 500 °C (ZNM500), X-ray diffraction (XRD) technique was used to determine what the changes were. On the other hand, the aforementioned samples were used to carry out the degradation of the Reactive Black 5 (RB5) textile dye, relying on a photocatalytic process. The effects of calcinations at 250 °C and 500°C on the materials, according to the diffraction patterns are: i) increase in the amorphous phase; ii) positive or negative shift (compared to ZNM025), of the diffraction peaks of ZNM250 and ZNM500; iii) decrease in particle size, according to the Debye-Scherrer model; iv) absence of diffraction peaks of Iron Oxide (FeOx) particles.

In addition, we have found that the sample set can photocatalytically mineralize the RB5 dye. The degree of mineralization was verified through the decrease in the height of the absorption band of the UV-Vis spectrum ( $\lambda = 600$  nm), which corresponds to the azo bond ( $-N=N-$ ) of the chemical structure of the compound. organic (RB5). Finally, the following dye degradation order was established,  $ZNM025 < ZNM250 < ZNM500$ , indicating that the heat treatment at 500 °C of natural clinoptilolite improves the catalytic properties and allows for better RB5 degradation efficiencies.

**Keywords:** Natural zeolite, Photocatalysis, X-rays

## INTRODUCTION

Zeolites are crystalline minerals; which are made up of a network of silicon and aluminum tetrahedrons (aluminosilicates), linked together by oxygen atoms  $[SiO_4]^{4-}$  y  $[AlO_4]^{5-}$  [1-3]; in their intramolecular structure

they have channels or cavities of molecular dimensions (30 to 150 nm) [4].

Natural zeolites (ZN) have been the subject of much research, due to their adsorbent properties, abundance, availability and their low cost compared to other minerals, but there is an important limitation, which are the impurities it has, the most common being the presence of iron oxides, which is associated with non-zeolitic phases, and other impurities found are cationic species [5].

Recently, at the XIX National Academic Meeting on Physics and Mathematics 2014, held at ESFM-IPN (Mexico City), preliminary results of the spectroscopic characterization of natural zeolites from Etlá, Oaxaca were presented with the following techniques: XRD (Diffraction of X-rays), UV-Vis (Ultraviolet-Visible Spectroscopy) and FTIR (Infrared Spectroscopy) [6]. It was found that for the diffraction peak at  $2\theta = 9.8$ , there is a decrease in its intensity, which is due to the heat treatment to which the sample was subjected; In addition, an average grain size was established by means of the Debye-Scherrer analytical method [7-9] from only this diffraction peak. In addition, in this work, using the FTIR-CO and UV-Vis techniques, the presence of iron oxide/hydroxide (FeOx) nanophases was determined in the zeolite with non-calcined three-hour grinding and the modification of these FeOx nanophases by calcination in an oxidizing atmosphere at temperatures of 250 and 500 °C, respectively. These FeOx nanophases were shown to have maghemite/magnetite type ferromagnetic characteristics. By heating these species above 500 °C, they transformed into a new hematite-type ferromagnetic nanophase [10,11].

In the previous work, the XRD peaks of the natural zeolite calcined at 250 and 500 °C, were analyzed, at the  $2\theta = 9.8$  peak; now, in this report, the Debye-Scherrer analysis is extended and quasi-overlapping diffraction

peaks are described in detail; two from the clinoptilolite phase, two from the mordenite phase and one associated with the quartz phase. In the second part of this work, the photo-catalytic degradation of the Reactive Black 5 (RB5) dye dissolved in deionized water is studied. The main objective is to find the average grain size of the three minerals, in addition to monitoring their photo-degrading activity on the organic azo compound, and to relate the influence of heat treatment on the catalytic properties of zeolitic powders.

## METHODOLOGY

The zeolitic mineral was extracted directly from the deposit of the town of ETLA, in the state of Oaxaca, in Mexico; its origin is natural since it was not subjected to no physicochemical process to remove undesirable impurities; its composition is approximately 75% of the clinoptilolite crystalline phase, the rest of the material is made up of mordenite, erionite, quartz, feldspar, iron oxides [12].

This material was submitted to a calcination process during an interval of 2 to 3 hours, maintaining a stable temperature of 250 and 500 °C respectively; The equipment used was a Thermolyne Sybron muffle model Programmable Asching Furnace Type 2000.

The X-ray measurements were carried out in a Rigaku Miniflex 600 model powder diffractometer, with a graphite monochromator and using CuK $\alpha$  radiation with a  $\lambda=0.154$  nm, a  $V=40$  kV, current of 15 mA; with a step increment of 0.001, and  $\omega=2^\circ/\text{min}$ . The equipment was provided by the Center for Nanosciences and Micro and Nanotechnologies (CNMN-IPN).

The photodegradation was carried out in a three-way reactor under the following conditions: 100 ppm of Black 5 dye diluted in distilled water were prepared; Subsequently, it was stored in a dark container (to avoid minimal contact with white light), a volume

of 250 ml of prepared liquid was measured and deposited in a reactor (which was covered with aluminum to block external light), and 50 mg of powdered zeolite were added, later 1.5 ml of HCl was added to control the pH of the solution and 0.5 ml of H<sub>2</sub>O<sub>2</sub> to start the reaction, a 13-watt visible light lamp (white light) was used to start with photocatalysis.

Photocatalytic measurements were quantified through UV-Vis spectroscopy; catalytic activity spectra were obtained by means of a Cary 1G model Variant UV/Vis lamp spectrophotometer with  $v=600$  nm/min as scanning speed; the wavelength range was  $\lambda=190$  to 800 nm. The reaction of photocatalysis was monitored from 0 to 200 min. An aliquot was taken at each 20 min interval to determine its corresponding UV-Vis spectrum. The experimentation was carried out in the G-bis Building of the UAM-Azcapotzalco.

## RESULTS Y DISCUSSION

### A. X-RAY DIFFRACTION

For the diffraction lines at  $2\theta=13.45$  and 19.61, of the mordenite phase; the diffractograms for the 3 samples (ZNM025, ZNM250 and ZNM500) were studied. In the Figure 1 schematizes the peak at 13.45, the corresponding peak at 19.61 (not shown).

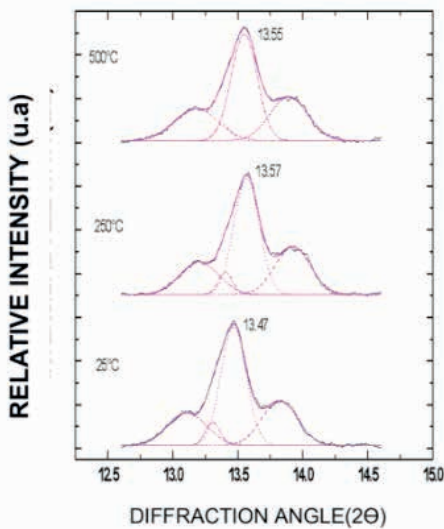


Figure 1. XRD simulation for the  $2\theta = 13.45$  peak for the samples ZNM025, ZNM250 and ZNM500, of the mordenite phase with 4 Gaussian distributions.

To better understand the impact of calcination temperature on zeolite powders; the average particle size was determined using the Debye-Scherrer equation [6, 13].

$$L = K \cdot \lambda / \beta \cos \theta \quad (1)$$

The variables correspond to:

$K = 0.89$  is a constant

$\lambda = 0.154$  nm

$\beta$  = Peak width in radians

$\theta$  = half angle of diffraction

The peak analyzed at  $2\theta = 13.45$  is surrounded by 2 neighboring peaks, one on its right side and the other on the left side, for this reason it is identified as a quasi-overlapping peak, for which there are several zeolitic phases present, but the peak is more defined (central band) is the one that is studied.

The following information is extracted from the study: the apparent center, its width, the height, the peak area, as well as the approximate diameter of the grain. The results were reported in Table I.

Sample	hkl	peak center	peak width	peak height	peak area	Particle diameter (nm)
ZNM025	111	13.47	0.196	5403.5	1325.9	40.35
ZNM250		13.57	0.194	5321.8	1296.2	40.72
ZNM500		13.55	0.200	4885.0	1223.9	39.55

TABLE I - Fit parameters of the four Gaussians of the peak at  $2\theta = 13.45$  to determine the particle diameter of the mordenite phase.

Regarding the clinoptilolite phase, the peaks at  $2\theta = 11.19$  and  $32.02$  were analyzed, in this section only the first peak is reported, see Figure 2.

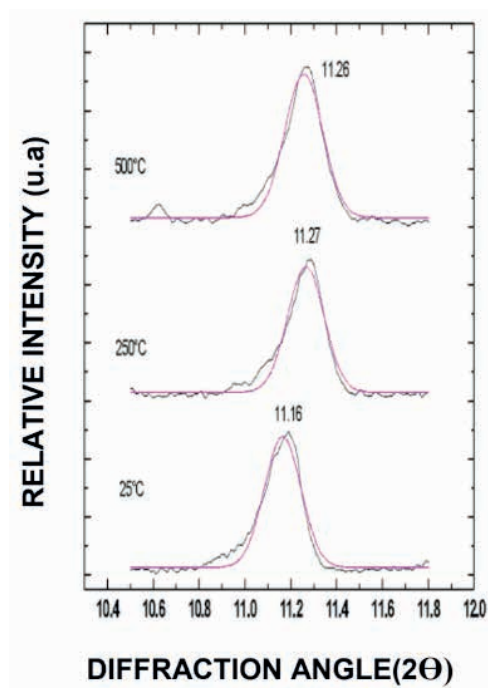


Figure 2. XRD simulation for the  $2\theta = 11.19$  peak for the samples ZNM025, ZNM250 and ZNM500, of the clinoptilolite phase with a Gaussian distribution.

It is notably appreciated that for the clinoptilolite phase its diffraction peak is uniform, and that there are no contiguous peaks that affect its behavior; For this reason, only one simulation is carried out, which allows a perfect fit and obtains reliable values. when there is an overlap of bands, a more

rigorous simulation is needed to have a finer fit.

As in the mordenite phase, the results found for the clinoptilolite phase are shown in Table II. This table allows us to observe in greater detail the changes produced in the 3 samples.

Sample	hkl	peak center	beak width	peak height	peak area	Particle diameter (nm)
ZNM025	200	11.16	0.160	2251.9	451.88	49.36
ZNM250		11.27	0.160	2163.5	434.37	49.19
ZNM500		11.26	0.166	2472.2	513.40	47.65

TABLE II - Parameters of the fit to a Gaussian of the peak at  $2\theta = 11.19$  to determine the particle diameter of the clinoptilolite phase.

Finally, a single peak of the  $\alpha$ -quartz phase was analyzed at  $2\theta=26.65$ , see Figure 3. In the Table III specifies all the information related to the  $\alpha$ -quartz phase.

The peak at  $2\theta=26.65$  has quasi overlap and therefore a Gaussian fit is needed to have a fine coupling.

Reference [14] shows the X-ray diffraction patterns of the phases: clinoptilolite, mordenite and  $\alpha$ -quartz, according to this, the peaks that were not superimposed were chosen, for this the simulation was carried out to find all the desired parameters.

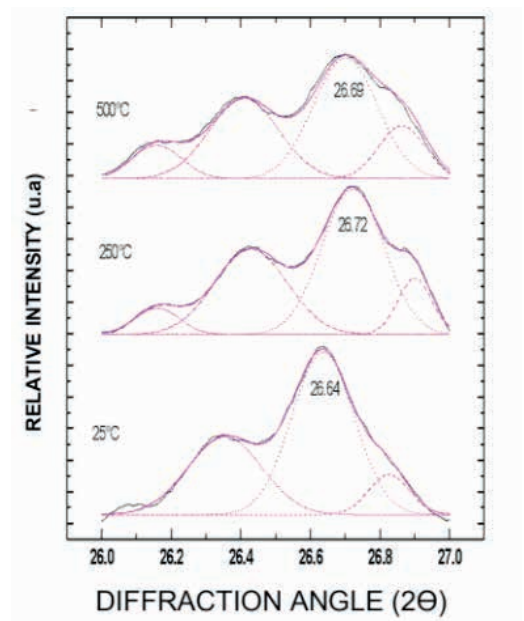


Figure 3. XRD simulation for the  $2\theta= 26.65$  peak for the samples ZNM025, ZNM250 and ZNM500, of the  $\alpha$ -quartz phase with 3 and 4 Gaussian distributions, respectively.

When analyzing Table I to III, the effect of calcination on the samples is reflected; although there was no significant change, in the center and in the width of the peaks; however, if there is considerable variation height, area, and diameter of the particle.

Sample	hkl	peak center	beak width	peak height	peak area	Particle diameter (nm)
ZNM025	101	26.64	0.179	10287	2306.4	45.14
ZNM250		26.72	0.179	9212.6	2061.7	45.15
ZNM500		26.69	0.186	7645.5	1779.2	43.48

TABLE III - Fitting parameters to three and four Gaussians, respectively, peak at  $2\theta = 26.65$ , to determine the particle diameter of the  $\alpha$ -quartz phase.

The general average diameter of the three phases of the zeolite under study is represented in Table IV.

Sample	Dp (nm) Clinoptilolite	Dp (nm) Mordenite	Dp (nm) $\alpha$ -Quartz
ZNM025	48.37	42.61	45.14
ZNM250	47.75	43.78	45.15
ZNM500	46.04	42.545	43.48

TABLE IV - Average diameter of the 3 zeolite phases at 3 different calcination temperatures.

The thermal effect on the material is constantly noted in the change in grain size; on the other hand, the initial diameter for the three phases is greater than the final diameter, according to the information provided; the following can be set:

$$Dp_{clinoptilolite} > Dp_{\alpha\text{-quartz}} > Dp_{mordenite} \quad (2)$$

## B. PHOTO-CATALYTIC ACTIVITY

Photocatalysis is an advanced oxidation process (POA) that employs a catalyst,  $H_2O_2$  and a light source (visible light); has the objective of mineralizing organic compounds from residual effluents [15]. The quantification of a photo-catalytic process can be carried out by: High Performance Liquid Chromatography (HPLC) [16], and controlling the absorption bands of the dye by UV-Vis Spectrophotometry [17, 18].

In this report we have used the monitoring of the band with a wavelength at 600 nm to determine the degree of degradation and discoloration of the Reactive Black 5 (RB5) compound.

RB5 is made up of a group of atoms, which are responsible for the characteristic color (black), known as chromophores; of which, the most common are: carbonyls ( $-C=O$ ), azo compounds ( $-N=N-$ ), methyls ( $-CH_3$ ), nitro groups ( $-NO_2$ ) and quinoid groups [19]; This dye is widely used in the textile industry, for the garment dyeing process, see Figure 4.

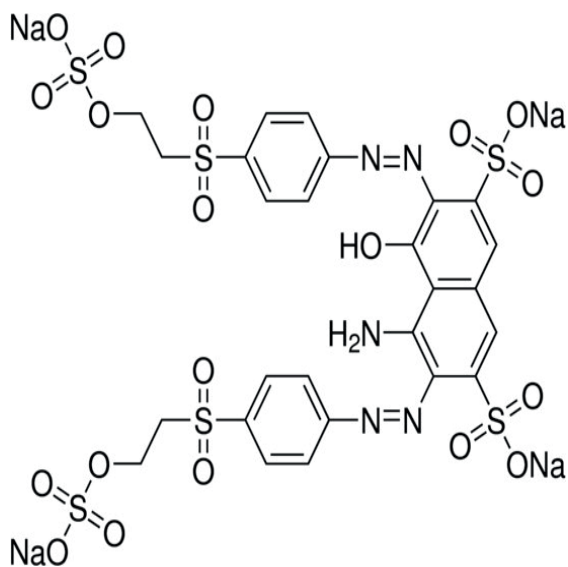


Figure 4. Molecular structure of Reactive Black 5 dye

Figure 5 shows the UV-Vis spectrum of RB5, in collaboration with the sample ZNM025 as a catalytic agent.

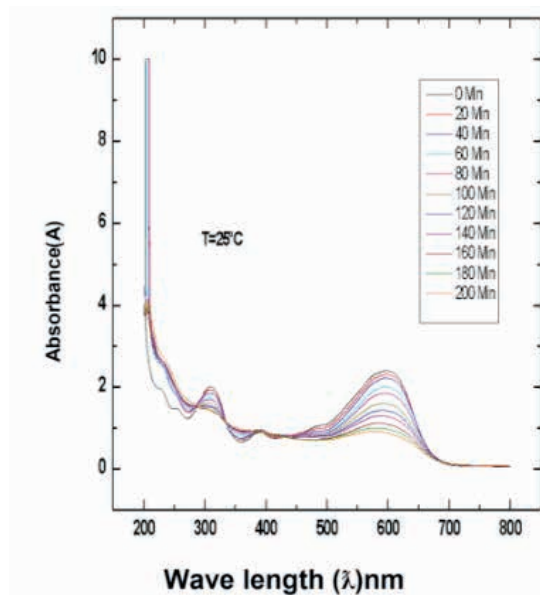


Figure 5. UV-Vis spectrum of RB5 degradation for an irradiation time of 200 min using ZNM025.

The initial absorption band at  $\lambda=600$  nm disappears as a function of the photocatalytic reaction time, that is, the zeolitic material (ZNM025) catalytically promotes the

degradation and discoloration of the organic compound, qualitatively it can be seen that it is a good catalyst.

The photodegrading behavior of the materials ZNM250 (Figure 6) and ZNM500 (Figure 7) on RB5 is shown below.

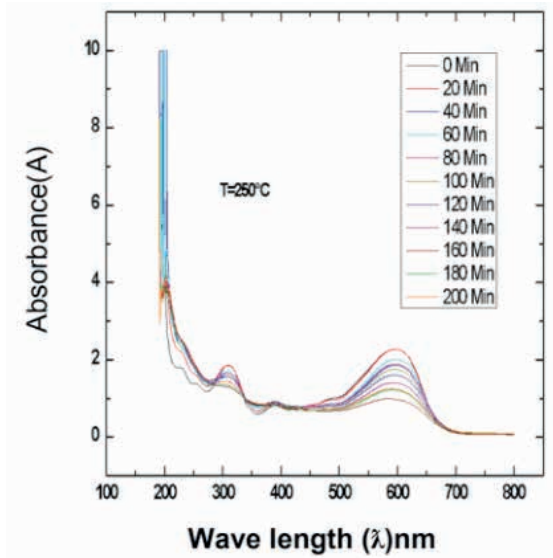


Figure 6. UV-Vis spectrum of RB5 degradation for an irradiation time of 200 min using ZNM250.

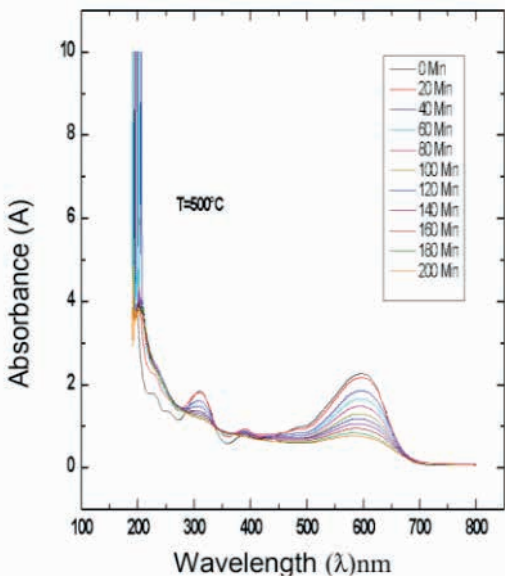


Figure 7. UV-Vis spectrum of RB5 degradation for an irradiation time of 200 min using ZNM500.

In the same way, both in Figure 6 and 7 it is observed that the absorption peaks decrease in intensity, this is due to the function that the calcined zeolitic mineral induces on the organic compound. Thus, it is observed that the heat treatment of the mineral allows there to be an improvement in the degradation and discoloration of RB5.

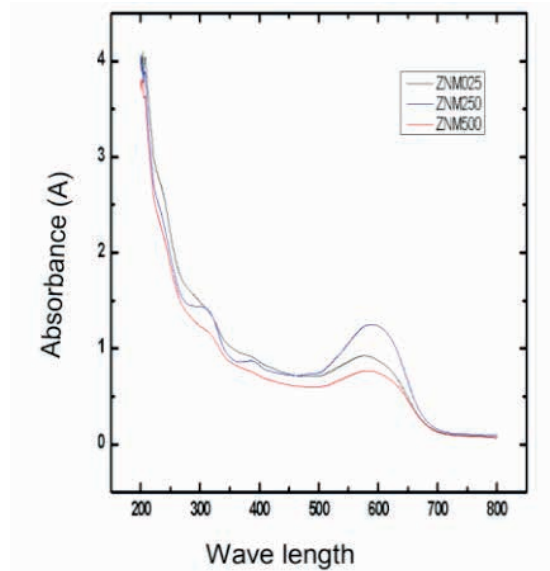


Figure 8. UV-Vis spectrum of total RB5 degradation using ZNM025, ZNM250 and ZNM500 respectively..

Now, Figure 8 presents the comparative analysis of the curves of the 3 spectra of Figures 5, 6 and 7 at 200 min of reaction; that is, the last curve (orange color) of the 3 UV-Vis spectra is extracted, the three final curves are all reflected in a general graph (see Figure 8). From which it is observed how when using calcined zeolites, they considerably attenuate the RB5 peaks ( $\lambda=600$  nm); qualitatively, it is established that the photo-degradation pattern follows this trend:

$$ZNM\ 500 > ZNM\ 025 > ZNM\ 250 \quad (3)$$

For a reaction time of 200 min, there is a good mineralization of the azo compound, possibly in  $CO_2$ , CO, carboxylic acids, etc., we can say that the 3 zeolites demonstrate their high catalytic power, but especially the

ZNM25 and ZNM500 samples. Although the reaction time is moderately long, in future works it is intended to make modifications to zeolites to improve the oxidation efficiency of RB5 in less time.

## CONCLUSIONS

The structural study using the XRD technique shows the presence of 3 different phases in the natural zeolite corresponding to mordenite, clinoptilolite and  $\alpha$ -quartz. When said material is subjected to a calcination process; a rearrangement of its crystallographic structure occurs, a modification in the grain size, as well as a change in its peak area.

When monitoring the intensity of the 600 nm peak of the RB5 dye, it is observed that the mineralizing photocatalytic activity is more efficient when the zeolite that was calcined at 500°C is occupied.

## ACKNOWLEDGMENTS

The authors thank Dr. José Alberto Andraca Adame from the CNMN-IPN for his support in the X-ray measurements.

We also thank Eng. Julio Cesar Espinoza Tapia from the UAM-Azcapotzalco for the technical support provided in the UV-Vis measurements.

This work has been sponsored by the IPN Research and Postgraduate Secretariat, projects SIP-20151252, SIP-20150742, and also by BEIFI-IPN and COFAA-IPN.

## REFERENCES

- [1] A. Dyer. An Introduction to zeolite molecular sieves, *John Willey and Sons*, New York, 1998.
- [2] O. E. Alcantara, C. Cheeseman, J. Knigh and M. Loizidou, "Properties of alkali-activated clinoptilolite", *Cement and Concrete Research*, 30, 1641-1646, 2000.
- [3] A. Al-Haddad, E. Chmielewská and S. Al-Radwan, "A brief comparable lab examination for oil refinery wastewater treatment using the zeolitic and carbonaceous adsorbents", *Petroleum & Coal*, 49(1), 21-26, 2007.
- [4] C. S. Cundy and P. A. Cox, "The hydrothermal synthesis of zeolites: History and development from the earliest days to the present time", *Chem Rev*, 103, 663-701, 2003.
- [5] D. Tito-Ferro, I. Rodríguez-Iznaga, B. Concepción-Rosabal, F. Chávez-Rivas, V. Córdova-Rodríguez y R. Rizo-Beyra, "Presence of iron in zeolitic rocks in Palmarito de Cauto deposit: separation and characterization of magnetic phases", *Minería y Geología*, 27(1), pp. 23-27, 2011.
- [6] G. Zacahua-Tlacuatl, J. J. Castro-Arellano, E. M. Lizarraga-Díaz, M. A. Sierra-Franco, G. Berlier, F. Chávez-Rivas, V. Petranovskii y S. Coluccia, "Estudio de Difracción de Rayos X y FTIR-CO de tobas zeolíticas naturales calcinadas, provenientes de Etila, Oaxaca" Reunión Nacional Académica de Física y Matemáticas, Ed. XIX, pp. 1-4, 2014.
- [7] Langford, J. I. and Wilson, A. J. C. *J. Appl. Crystallogr.* 11, 102-113 (1978).
- [8] Cullity, B. D. *Elements of X-ray Diffraction* 2<sup>nd</sup> Ed. (Addison-Wesley, 1978).
- [9] Warren, B. D. *X-ray Diffraction* 2<sup>nd</sup> Ed. (Dover, 1990).

- [10] M. Mihaylov, E. Ivanova, K. Chakarova, P. Novachka and K. Hadjiivanov, "Reduced iron sites in Fe-BEA and Fe-ZSM-5 zeolites: FTIR study of CO adsorption and  $^{12}\text{C}^{16}\text{O}$ - $^{13}\text{C}^{18}\text{O}$  CO-adsorption" *Applied Catalysis A: General*, vol.391, pp. 307-511, 2002.
- [11] C. Lemire, R. Meyer, V. E. Henrich, Sh. Shaikhutdinov and H. J. Freund, "The surface structure of  $\text{Fe}_3\text{O}_4$  (111) films as studied by CO adsorption", *Surface Science*, vol. 572, pp. 103-114, 2004.
- [12] G. Zacahua-Tlacuatl, PhD. Thesis in Chemical Engineering, National Polytechnic Institute, México D.F., 2011.
- [13] M. Khatamian and M. Irani, "Preparation and characterization of nanosized ZSM-5 zeolite using kaolin and investigation of kaolin content, crystallization time and temperature changes on the size and crystallinity of products", *J. Iran. Chem. Soc.*, Vol.6, No. 1, March 2009, pp. 187-194.
- [14] M. M. J. Tracy and J. B. Jiggins, "Collection of simulated XRD powder patterns for zeolites" *Structure Commission of the International Zeolite Association*, Fourth Revised Edition, 2001.
- [15] E. Gil-Pavas, L. Quintero-Olaya, M. Rincón-Uribe y D. Rivera-Agudelo, "Degradacion de colorantes de aguas residuales empleando  $\text{UV}/\text{TiO}_2/\text{H}_2\text{O}_2/\text{Fe}^{2+}$ " *Universidad Eafit*, Vol. 43, No. 146, pp. 80-101, 2007.
- [16] S. Fukahori, H. Ichiura, T. Kitaoka and H. Tanaka, *Appl. Catal.*, B 2003, 43, 453.
- [17] C. J. Ferrusquía-García, G. Roa-Morales, M. M. García-Fabila, A. Amaya-Chávez y T. B. Pavón-Silva, "Evaluación de la degradación de metil paratión en solución usando fotocatalisis heterogénea" *Revista Latinoamericana de Recursos Naturales*, 4 (2), pp. 285 – 290, 2008.
- [18] Luis F. Gómez y Víctor M. Sarria, "Fotodegradación heterogénea de Bisfenol A en agua con Dióxido de Titanio" *Quim. Nova*, Vol. 32, No. 5, 1164 – 1169, 2009.
- [19] A. Fernández-Alba, P. Letón García, R. Rosal García, M. Dorado Valiño, S. Villar Fernández y J. M. Sanz García, "Tratamientos avanzados de aguas residuales industriales, informe de vigilancia tecnológica", Fundación para el conocimiento Madrid CEIM, Cap. 2, pp. 16, 2006.